Journal of the European Ceramic Society 17 (1997) 719–725
© 1997 Elsevier Science Limited
Printed in Great Britain. All rights reserved
0955-2219/97/$17.00
PII: S0955-2219(96)00091-X

Anisotropic Grain Growth in α-Fe_2O_3-Doped Alumina

J. Tartaj* & G. L. Messing

Particulate Materials Center, Pennsylvania State University, University Park, PA 16802, USA

(Received 28 February 1996; revised version received 15 April 1996; accepted 3 May 1996)

Abstract

Addition of α-Fe_2O_3 seed particles to alkoxide-derived boehmite sols results in the development of a highly uniform and dense microstructure at 1300°C. Higher temperature treatments promote anisotropic grain growth of lath-like α-Al_2O_3 grains. The fundamental explanation for this is basically attributed to the presence of Fe^{2+} significantly improving the mass transport. By controlling time, sintering temperature and atmosphere conditions, it is possible to obtain an appropriate microstructural development that may lead to a new class of tough ceramic materials. © 1997 Elsevier Science Limited. All rights reserved.

1 Introduction

Grain growth in polycrystalline alumina has been studied extensively because of the impact of the microstructure on properties. Grain growth depends on several factors such as purity, heat treatment, grain size, size distribution, grain morphology, interfacial energy and the presence of second phases. On the other hand, small amounts of dopants can have a significant effect on grain growth. For example, the addition of MgO[1,2] reduces abnormal grain growth in Al_2O_3 for reasons that are still in dispute. Oxides of Ti, Mn, Nb, Cu and Ge[3] increase the grain growth rate in alumina. Increased growth rates have been attributed to increased material transport as a result of strain in the aluminium lattice, the presence of a glassy phase, and increased grain boundary or surface diffusion. Manganese oxide, ferric oxide and titania[4,5] have been reported to promote the formation of platelet-shaped or anisotropic grains as a result of differences in the growth rates of the bounding interfaces. The fundamental explanation for anisotropic grain growth in alumina is not totally understood but includes several proposals: an inhomogeneous distribution of the dopant[2,6] and the presence of a liquid phase on the grain boundary.[7] In the case of ferric oxide, if the Al_2O_3–Fe_2O_3 system[8] is sufficiently pure, a liquid phase should not be present in air. The effect of iron doping on alumina grain growth has also been studied in terms of defect structure and diffusional processes. Several studies report[9,10] that the diffusion coefficients increase with decreasing oxygen pressure, and this enhanced diffusivity may be attributed to the presence of Fe^{2+}. If Fe^{2+} is present, positive defects must form to maintain electrical neutrality, interstitial aluminium and oxygen ion vacancies; in this way, the mass transport is improved.

The aim of this work is to gain knowledge and control of the factors that affect the anisotropy of grain growth, using ferric oxide as a dopant. To study exclusively the effect of the iron in this process, high-purity alumina was synthesized.

2 Experimental Procedure

2.1 Preparation of boehmite sol

High-purity boehmite was synthesized by hydrolysis of aluminium trisec-butoxide. The alkoxide was added with vigorous stirring to distilled water maintained at 80–90°C. To prevent premature hydrolysis, the viscous alkoxide was transferred directly from its container under dry nitrogen using a peristaltic pump, from inside a nitrogen-purged glove box. Nitric acid was added to stabilize the sol at pH ≈ 3. The slurry was then transferred to a reflux apparatus, where the temperature was maintained at ~95°C under gentle stirring. The dispersed sol was kept in these conditions for 10 days, after which the sol was fully transparent.

---

*Permanent address: Department of Electroceramic, Instituto de Cerámica y Vidrio, (CSIC), 28500 Arganda del Rey (Madrid), Spain.

2.2 Preparation of α-Fe$_2$O$_3$ seed particles

An aqueous solution of 0·15 M Fe(NO$_3$)$_3$.9H$_2$O was precipitated with an excess of NH$_4$OH under vigorous stirring. The precipitate was repeatedly washed and centrifuged and then redispersed in water at pH ≈ 3 adjusted by HNO$_3$. The sol was refluxed with constant stirring at ~90°C for 3 days. After refluxing the sol was dried and the powder was characterized by X-ray diffraction (XRD) and differential thermal analysis (DTA), and the particle size distribution was determined by light scattering (L900-Horiba).

2.3 Preparation of seeded boehmite sols

Seeded boehmite sols were prepared by adding the α-Fe$_2$O$_3$ sol in appropriate proportions to obtain a seed particle number concentration of 10^{12}–10^{14} seed particles per cm^3 of α-Al$_2$O$_3$. Sol mixtures were concentrated at 65°C under vacuum in a rotary evaporator to a viscosity near the gel point. Gel monoliths of 1 cm^2 and 500 μm thickness were cast in plastic beakers and allowed to dry for several days at room temperature. To determine the onset temperature of the θ-Al$_2$O$_3$ $\rightarrow$ α-Al$_2$O$_3$ transformation by DTA, dry powders were heated at 10°C min^{-1} in air. For sintering, the monoliths were thermally treated at temperatures up to 1500°C for 0·5 to 3 h. Sintered densities were measured by Archimedes' technique using distilled water.

3 Results and Discussion

3.1 Preliminary results

XRD peaks of the seed sol dried at 100°C correspond to γ-FeO(OH) (goethite). Heating the goethite at 10°C min^{-1} leads to the formation of α-Fe$_2$O$_3$, haematite, at 600°C. The median diameter of the goethite particles is ≈ 90 nm and 90% of the particles are between 80 and 110 nm. From the sol solids content and the number frequency of particle size distribution, the number of particles of α-Fe$_2$O$_3$ per cm^3 of α-Al$_2$O$_3$ was calculated. The $\theta \rightarrow \alpha$-Al$_2O_3$ transformation temperature is shown in Table 1 for various Fe$_2$O$_3$ seed concentrations.

Table 1. Effect of Fe$_2$O$_3$ additions on the $\theta \rightarrow \alpha$-Al$_2O_3$ transformation temperature

Number of α-Fe$_2$O$_3$ particles per cm^3 of α-Al$_2$O$_3$	*Temperature (°C)*
Al$_2$O$_3$ (0 wt%)	1215
10^{12} α-Fe$_2$O$_3$/cm^3 (0·1 wt%)	1143
5×10^{12} α-Fe$_2$O$_3$/cm^3 (0·4 wt%)	1134
10^{13} α-Fe$_2$O$_3$/cm^3 (0·8 wt%)	1122
5×10^{13} α=Fe$_2$O$_3$/cm^3 (4 wt%)	1084
10^{14} α-Fe$_2$O$_3$/cm^3 (8 wt%)	1067

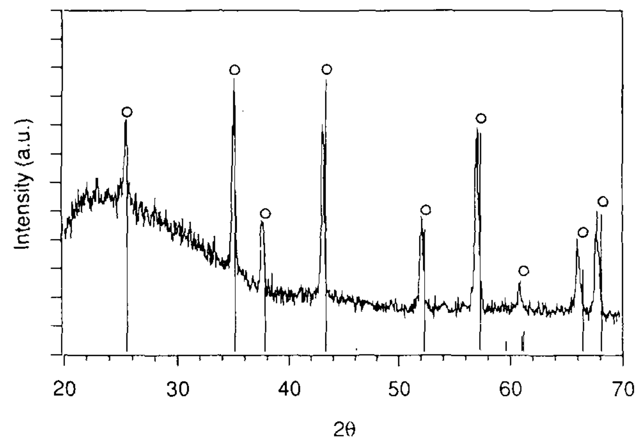

Fig. 1. X-ray diffraction pattern from 10^{14} α-Fe$_2$O$_3$ seeded alumina heated at 1200°C for 1 h in air. ○, α-Al$_2$O$_3$.

The unseeded boehmite transforms to α-Al$_2$O$_3$ at ~1215°C. Additions of 10^{14}/cm^3 α-Fe$_2$O$_3$ particles reduced the peak temperature to 1067°C. McArdle and Messing[11,12] attributed this reduced transformation temperature to the reduced nucleation barrier as a result of heterogeneous nucleation on the surface of the seed particles. In the XRD analysis corresponding to 10^{14}/cm^3 seeded alumina heated at 1200°C, Fig. 1, the alumina peaks are shifted because the Fe$_2$O$_3$ forms a complete solid solution with alumina and no Fe$_2$O$_3$ was detected. According to the phase diagram, α-Al$_2$O$_3$ can absorb up to 12 wt% Fe$_2$O$_3$ in this temperature range.[13]

The density measurements also confirmed a significant difference between the unseeded and seeded aluminas. The seeded samples reach full density at 1300°C, whereas the density of unseeded alumina is only 80%. The excellent densification behaviour of the seeded samples is a result of the uniform fine-grained microstructure that is developed during the seeded transformation.

3.2 Bulk microstructure development

The samples were polished and then thermally etched at 50°C below the sintering temperature for 30 min. The samples for scanning electron microscopy (SEM) were then gold-coated prior to examination. Microstructural development in unseeded and α-Fe$_2$O$_3$ seeded alumina gels is shown in Fig. 2 for sintering times of 2 h and temperatures of 1300°C in air. The unseeded and seeded samples with a low number concentration of seeds (10^{12}, 10^{13}) show the characteristic vermicular grain structure of α-Al$_2$O$_3$. In contrast, samples seeded with 10^{14} seeds develop a dense microstructure with a uniform grain structure of equiaxed and faceted grains. McArdle and Messing[11,12] explain this difference in microstructural development on the effect of nucleation frequency.

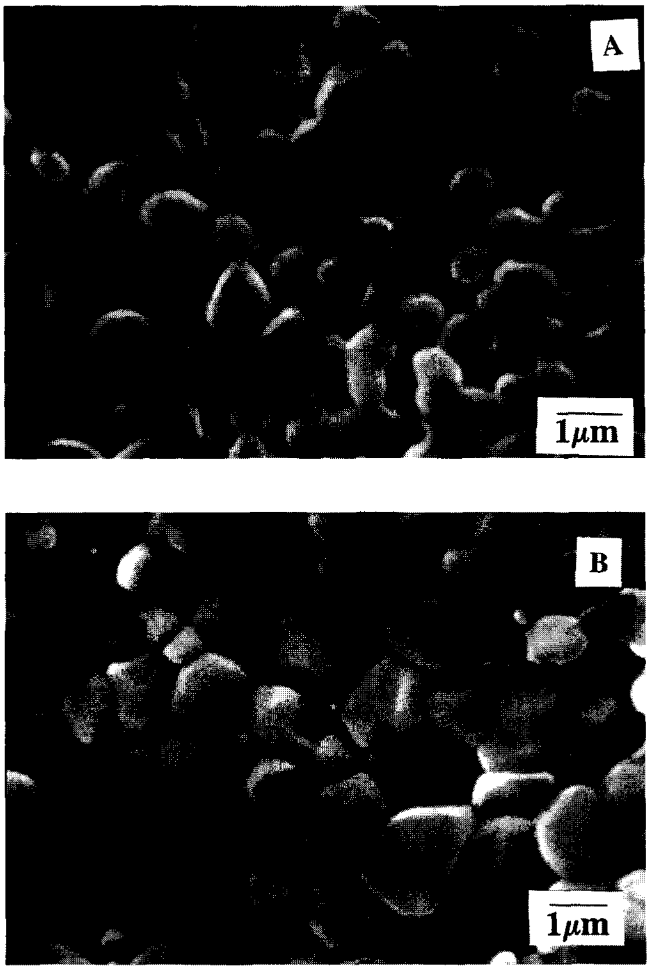

Fig. 2. Microstructure development of unseeded (A) and 10^{14} α-Fe_2O_3 seeded (B) alumina gels, sintered for 2 h at 1300°C in air.

The samples containing 8 wt% α-Fe_2O_3 were heated in air between 1450 and 1500°C for 0·5 to 3 h, Fig. 3. The samples heated at 1450°C start to develop a bimodal microstructure with large grains in a matrix consisting of finer grains. This fact is especially evident in samples heated at 1475 and 1500°C. As seen in Fig. 4, the aspect ratio of samples heated at 1475 and 1500°C decreases with increasing time. During growth the grains impinge on one another, and further growth results in a decrease in the aspect ratio of the anisotropic grains. The pores found inside the large grains could be due, if O_2 is released, to the gas evolution.

To determine the mechanism of anisotropic grain growth in Fe_2O_3-doped Al_2O_3 it is important to understand the grain boundary chemistry. Dufek *et al.*[14] report no preference for Fe^{3+} segregation in high-purity alumina containing 3·0% haematite and Sabol[15] reports, in samples of the same nature, no significant differences in the iron concentration between grain interiors, grain boundaries and triple points. Furthermore, no evidence of an intergranular glass phase could be seen, and the grain boundaries appeared free of any second phases. Analysis of samples by energy-dispersive spectroscopy (EDS) and electron microprobe analysis (EMPA) verifies these results. Therefore, we could conclude from these first results that chemical segregation to the grain boundary is not responsible for the development of anisometric grains; however, the evidence shows that the formation of anisometric grains is a result of the iron content. Therefore, it is necessary to further consider the role of the iron atoms. Previously, it was reported that diffusion coefficients calculated from sintering equations increased with increasing Fe addition and decreasing oxygen pressure. The oxygen partial pressure effect suggests that Fe^{2+} is responsible for this enhanced diffusivity.

To examine the role of Fe^{2+} on the anisotropic grain growth, alumina samples containing 4 wt% α-Fe_2O_3 were sintered in flowing argon. Sintering at 1500°C (2 h) reduced a significant fraction of the Fe^{3+} ions to Fe^{2+}, as indicated by the dark green colour of the samples after sintering in contrast with the light brown samples sintered in air. From thermodynamic equations developed by Kroger and co-workers[16,17] and from the Fe_2O_3–Al_2O_3 phase diagram, it is predicted that at least 30 wt% of the Fe^{3+} was reduced to Fe^{2+} in argon. The microstructural development in samples containing 4 wt% of α-Fe_2O_3 treated in air and in flowing pure argon is compared in Fig. 5. The sample sintered in air at 1500°C developed a uniform grain structure with equiaxed grains of between 1 and 3 μm. In contrast, the same sample sintered under flowing argon developed a bimodal microstructure with large and elongated grains and finer grains distributed between them. The microstructure contains a second phase mainly localized in the grain boundary. Chemical analysis of this phase by EDS on SEM, Fig. 6, indicates a high amount of Fe relative to inside the grain. X-ray diffraction analysis, Fig. 7, shows some small peaks that correspond to $FeAl_2O_4$ spinel. XRD analysis of samples seeded with 8 wt% Fe_2O_3 clearly shows the presence of $FeAl_2O_4$ as a secondary phase. These results indicate that the Fe^{3+} is reduced to Fe^{2+} and that it segregates to the grain boundary. Zhao and Harmer[18] suggest that this second phase could greatly assist in sintering and creep resistance by pinning grain boundaries and by accommodating grain-boundary sliding at triple points.

We propose that diffusive mass transport has been improved, and can be attributed to the presence of high Fe^{2+} concentration. The reduction of Fe^{3+} to Fe^{2+} produces, in order to maintain electrical neutrality of the crystal, oxygen ion vacancies and interstitial aluminium as described in eqns (1) and (2).[10,19] There is a significant driving force for segregation of Fe^{2+} at the grain boundaries, because

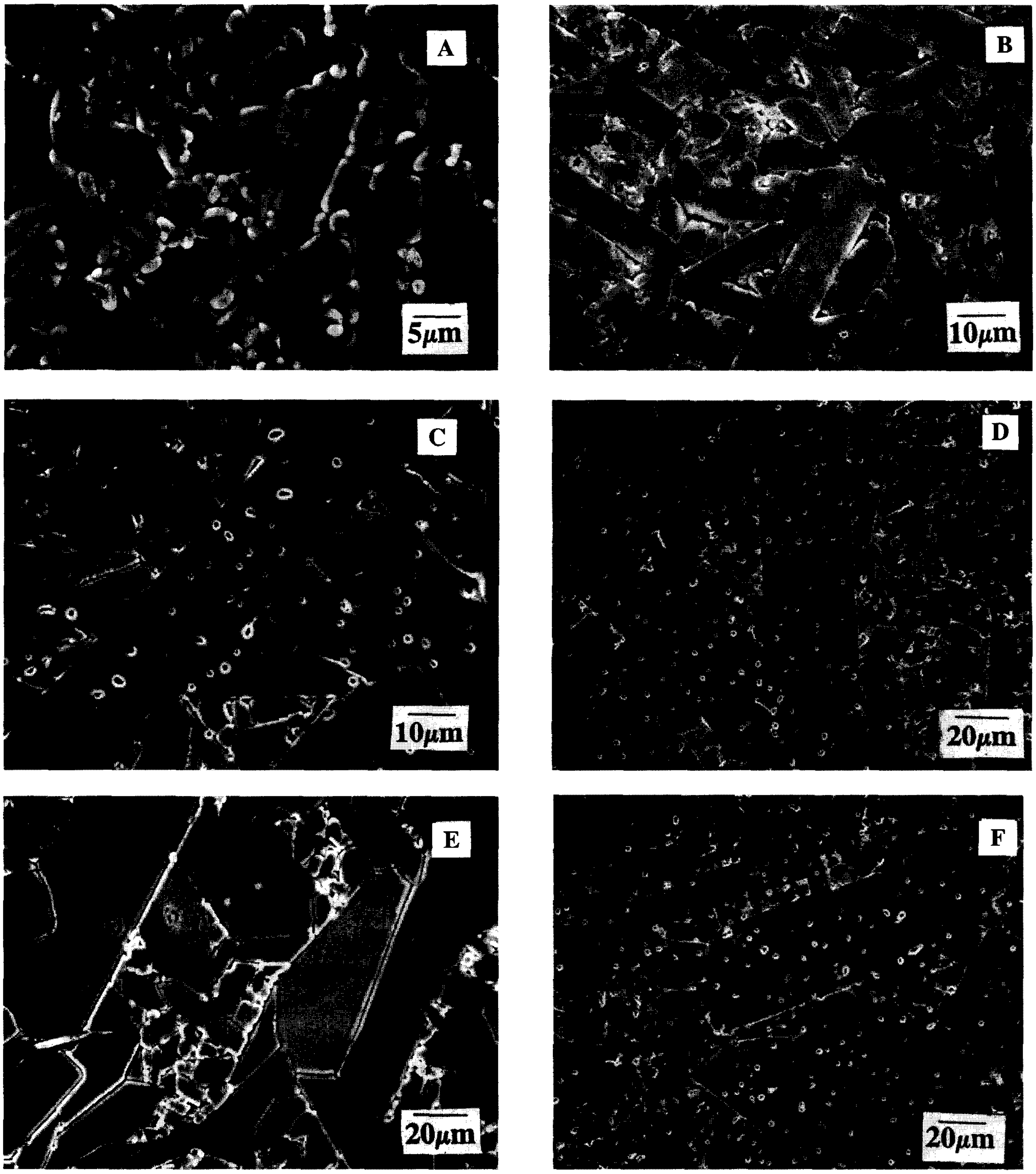

Fig. 3. Microstructure development of 8 wt% α-Fe_2O_3-doped alumina gels sintered in air at temperatures between 1450 and 1500°C: (A) 1450°C (2 h); (B) 1475°C (0·5 h); (C) 1475°C (1 h); (D) 1500°C (1 h); (E) 1500°C (2 h); (F) 1500°C (3 h).

the solubility of Fe^{2+} in Al_2O_3 is 0·7 to 1·9% at 1450°C.[8] It is suggested that grain boundary segregation of Fe^{2+} to high-energy nonbasal grain boundaries enhances the grain boundary diffusivity, resulting in rapid growth. Gordon and Ikuma[20] reported that the presence of iron in alumina increases the grain boundary diffusivity and that the diffusivity increases with decreasing oxygen partial pressure, suggesting that the diffusivity is related to the Fe^{2+} content at the grain boundary.

$$O_O^* + 2Fe_{Al}^* = 2Fe'_{Al} + V_O^{\cdot\cdot} + 1/2O_2(g) \quad (1)$$

$$3O_O^* + 2Al_{Al}^* + 6Fe_{Al}^* + 2V_i = 6Fe'_{Al} + 2Al_i^{\cdot\cdot\cdot} + 3/2O_2(g) \quad (2)$$

As previously reported, no secondary phases were detected in the grain boundary in 8 wt% Fe_2O_3 samples treated in air. However, anisotropic grains were clearly detected at temperatures ≥ 1450°C. This can be attributed to the dependence of the concentration of Fe^{2+} on temperature.

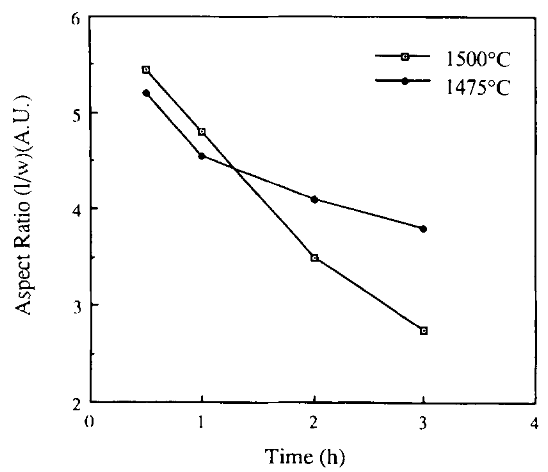

Fig. 4. Aspect ratio evolution of 8 wt% α-Fe_2O_3-doped alumina gels sintered in air at 1475b and 1500°C.

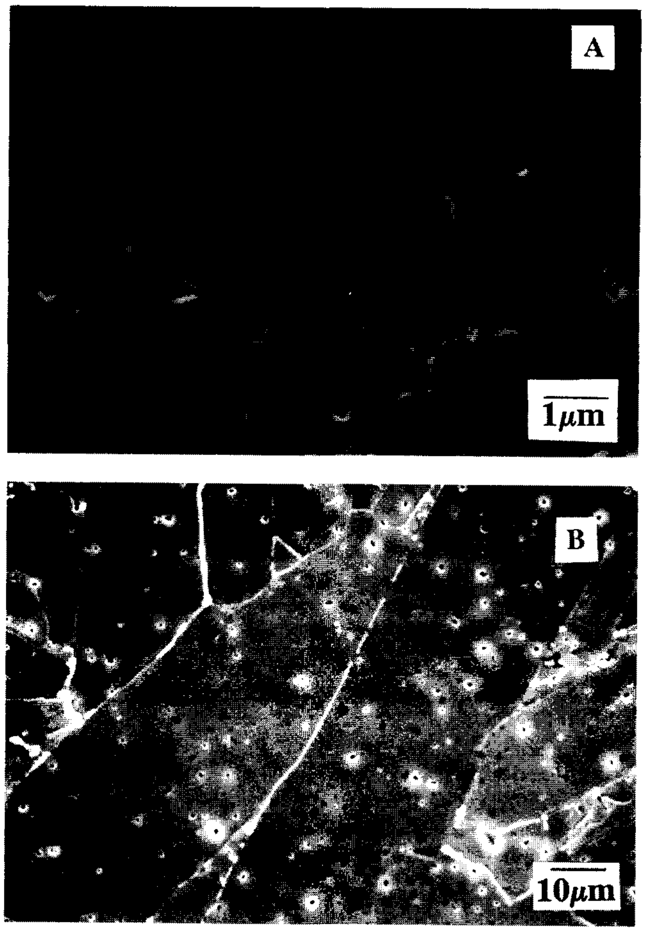

Fig. 5. Microstructure development by SEM of 4 wt% α-Fe_2O_3-doped alumina sintered at 1500°C for 2 h in air (A) and argon (B).

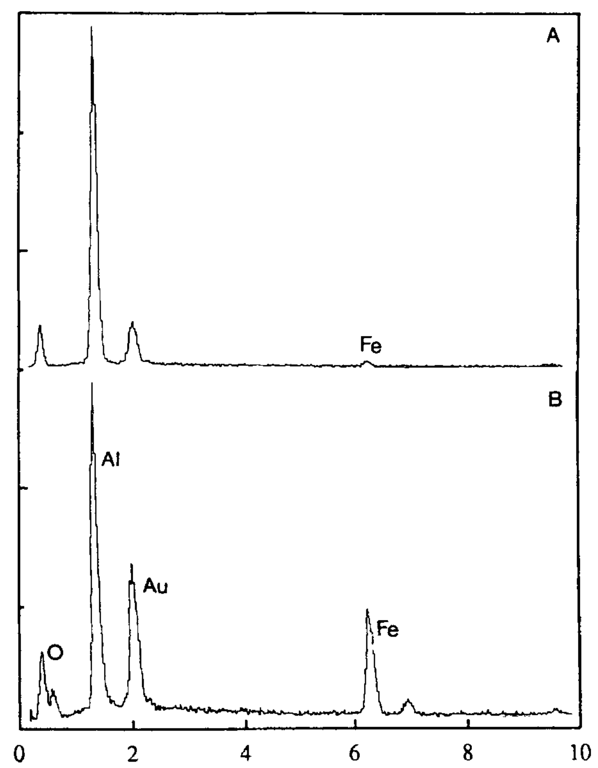

Fig. 6. Grain (A) and grain boundary (B) chemical analysis by EDS on SEM of 4 wt% α-Fe_2O_3-doped alumina sintered at 1500°C for 2 h in argon.

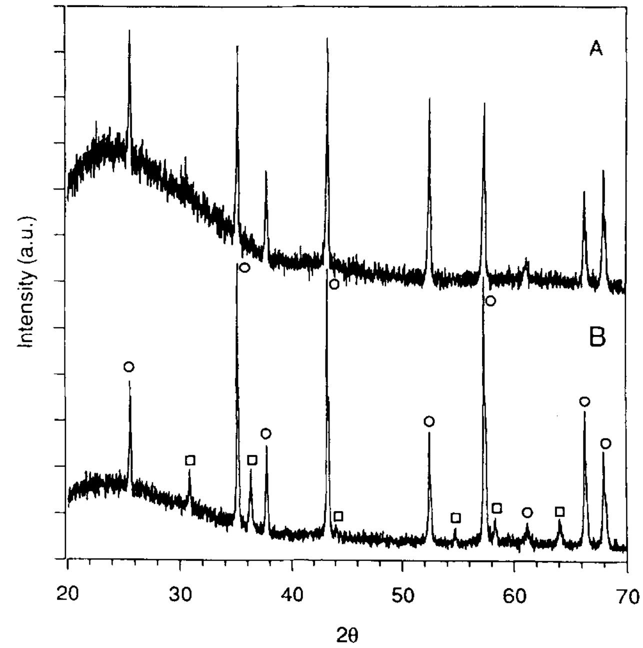

Fig. 7. X-ray diffraction patterns of (A) 4 wt% and (B) 8 wt% α-Fe_2O_3-doped alumina sintered at 1500°C for 2 h in argon. ○, α-Al_2O_3; □, $FeAl_2O_4$.

Phillips and Muan[21] reported that Fe_2O_3 heated in air loses oxygen at 1388°C. At 1450°C in air, iron is primarily in the trivalent state, and only 2% of the total Fe^{3+} is reduced.[22] This amount of Fe^{2+} in the case of the highest iron concentration is probably sufficient to promote anisotropic grain growth, but it is below the chemical detection limit. The green colour of this sample indicates that Fe^{2+} is formed.[22] In samples with only 4 wt% Fe_2O_3 and heated at 1500°C in air, probably the amount of Fe^{3+} reduced is not sufficient to promote this anisotropic grain growth, so sintering in inert atmosphere or increased sintering temperature (1650°C) is necessary to increase the amount of Fe^{2+} and promote the anisotropic grain growth. Figure 8 shows the distribution of the iron in the

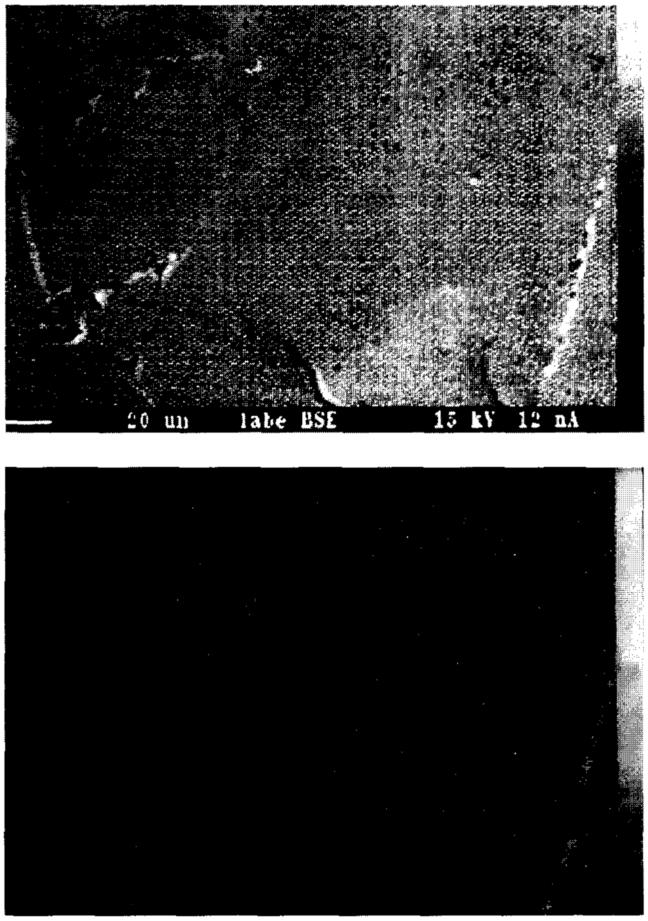

Fig. 8. Microstructure development by SEM and Fe distribution by EMPA of 4 wt% α-Fe_2O_3-doped alumina sintered at 1650°C for 2 h in air.

corresponding microstructure obtained by EMPA in a 4 wt% Fe_2O_3 sample sintered at 1650°C in air. Clearly, a higher iron concentration is detected in the grain boundary. The quantitative analysis shows that 15% of the total iron is segregated to the grain boundary.

So, by controlling time, sintering temperature and atmosphere conditions, it is possible to obtain very different microstructures and such control could be very interesting in the design of materials for special uses. In this way, 8 wt% Fe_2O_3-doped samples sintered in air at 1475 and 1500°C permit one to obtain bimodal microstructures with anisotropic grains and appropriate aspect ratio by controlling the sintering time. In this case ~2% of total iron is reduced to Fe^{2+}, below the solubility limit, therefore a mechanism based on the creation of oxygen vacancies could explain the enhanced grain growth process, and the pores inside the grains could be evidence to support this. In contrast, sintering in inert atmosphere or increased sintering temperature up to 1650°C reduces a significant amount of Fe^{3+}, producing an evident segregation of Fe^{2+} to the grain boundary resulting to an exaggerated grain growth.

4 Conclusions

The addition of α-Fe_2O_3 seed particles to alkoxide-derived boehmite sols is very effective in reducing the $\theta \rightarrow \alpha$-$Al_2O_3$ transformation temperature, preventing the development of vermicular pore structure and permitting complete densification of boehmite at 1300°C, as a result of the uniform, fine-grained microstructure that is developed during transformation. Higher temperature treatment promotes anisotropic grain growth of α-Al_2O_3 lath-like grains. The fundamental explanation for this is basically attributed to the presence of Fe^{2+}, the creation of oxygen vacancies and grain boundary segregation of Fe^{2+} to high-energy nonbasal grain boundaries resulting in rapid growth. By controlling time, sintering temperature and atmosphere conditions it is possible to obtain different microstructural development. Such control is interesting in the design of materials with a particular microstructure and may lead to a new class of tough ceramic materials, since it allows the *in situ* development of a self-reinforcing phase in the microstructure.

Acknowledgements

J. Tartaj thanks the NATO Program and MEC for a scholarship during the period when this work was carried out. Thanks are also extended to Professor P. Duran for helpful discussions.

References

1. Handwerker, C. A., Morris, P. A. & Coble, R. L., Effect of chemical inhomogeneities on grain growth and microstructure in Al_2O_3. *J. Am. Ceram. Soc.*, **72**[1] (1989) 130–136.
2. Bennison, S. J. & Harmer, M. P., Effect of MgO solute on kinetics of grain growth in Al_2O_3. *J. Am. Ceram. Soc.*, **66**[5] (1983) C90–C92.
3. Smothers, W. J. & Reynolds, H. J., Sintering and grain growth in alumina. *J. Am. Ceram. Soc.*, **37**[12] (1954) 588–595.
4. Cahoon, H. P. & Christenson, C. J., Sintering and grain growth of alpha-alumina. *J. Am. Ceram. Soc.*, **39**[10] (1956) 337–344.
5. Horn, D. S. & Messing, G. L., Anisotrophic grain growth in TiO_2-doped alumina. *Mat. Sci Eng.*, **A195** (1995) 169–178.
6. Lee, H. Y. & Kang, S. J. L., Chemically induced grain boundary migration and recrystallization in Al_2O_3. *Acta Metall. Mater.*, **38**[7] (1990) 1307–1312.
7. Kaysser, A. W., Sprissler, M., Handwerker, C. A. & Blendell, J. E., Effect of a liquid phase on the morphology of grain growth in alumina. *J. Am. Ceram. Soc.*, **70**[5] (1987) 339–343.
8. Muan, A., On the stability of the phase Fe_2O_3–Al_2O_3. *Am. J. Sci.*, **256**[6] (1958) 413–422.
9. Rao, W. R. & Cutler, I. B., Effect of iron oxide on the sintering kinetics of Al_2O_3. *J. Am. Ceram. Soc.*, **56**[11] (1973) 588–593.

0. Dorre, E. & Hubner, H., Alumina. In *Materials Research and Engineering*, ed. B. Ilschner & N. J. Grant. Springer-Verlag, Berlin–Heidelberg–New York–Tokyo, 1984, pp. 16–40.

1. McArdle, J. L. & Messing, G. L., Transformation and microstructure control in boehmite-derived alumina by ferric oxide seeding. *Adv. Ceram. Mater.*, **3**[4] (1988) 387–392.

12. McArdle, J. L. & Messing, G. L., Transformation, microstructure development, and densification in α-Fe_2O_3 seeded boehmite-derived alumina. *J. Am. Ceram. Soc.*, **76**[1] (1993) 214–222.

13. Atlas, L. M. & Sumida, W. K., Solidus, subsolidus, and subdissociation phase equilibria in the system Fe–Al–O. *J. Am. Ceram. Soc.*, **41**[5] (1958) 150–160.

14. Dufek, G., Vendl, A., Wrub, W. & Kieffer, R., Bestimmung der Verteilung von Sinterzusatzen in gesinterter Tonerde durch Mikrosondenanalyse (Determination of the distribution of sinter-additives in kaolin-sintered with a ultrasonic-analysis). *Ber. Dt. Keram. Ges.*, **53**[10] (1976) 336–338.

15. Sabol, S. M., Development of a textured and tabular grain microstructure in alumina fibers via seeded sol–gel processing. PhD Thesis, The Pennsylvania State University, University Park, PA, 1994.

16. Wang, H. A. & Kroger, F. A., Chemical diffusion in polycrystalline Al_2O_3. *J. Am. Ceram. Soc.*, **63**[11–12] (1980) 613–619.

17. Dutt, B. V. & Kroger, F. A., High-temperature defect structure of iron-doped α-alumina. *J. Am. Ceram. Soc.*, **58**[12] (1975) 474–476.

18. Zhao, J. & Harmer, M. P., Sintering of ultra-high-purity alumina doped simultaneously with MgO and FeO. *J. Am. Ceram. Soc.*, **70**[12] (1987) 860–866.

19. Gordon, R. S., Understanding defect structure and mass transport in polycrystalline Al_2O_3 and MgO via the study of diffusional creep. In *Advances in Ceramics*, ed. W. D. Kingery. American Ceramic Society, Columbus, OH, 1984, vol. 10, pp. 418–437.

20. Gordon, R. S. & Ikuma, Y., Creep of doped polycrystalline magnesium and aluminum oxides. In *Deformation of Ceramics Materials II*, eds R. E. Tressler & R. C. Brandt. Plenum Press, New York, 1984, pp. 341–352.

21. Phillips, B. & Muan, A., Stability relations of iron oxides: phase equilibria in the system Fe_3O_4–Fe_2O_3 at oxygen pressures up to 45 atmospheres. *J. Phys. Chem.*, **64** (1960) 1451–1453.

22. Ikuma, Y. & Gordon, R. S., Effect of doping simultaneously with iron and titanium on the diffusional creep of polycrystalline Al_2O_3. *J. Am. Ceram. Soc.*, **66**[2] (1983) 139–147.